Umudike Journal of Engineering and Technology (UJET); Vol. 9, No. 1, June 2023, pp. 26 – 36; Michael Okpara University of Agriculture, Umudike, Print ISSN: 2536-7404, Electronic ISSN:2545-5257; http://ujetmoua.com; https://doi.org/10.33922/j.ujet_v9i1_4

DEVELOPMENT OF THE FLOW PATTERN MAP FOR THE APPLICATION OF CO_2 GAS IN A THREE-PHASE DOWNWARD FLOW

Ntunde, D. I.

Department of Mechanical Engineering,
Michael Okpara University of Agriculture, Umudike, Nigeria
(Email: ntunde.dilibe@mouau.edu.ng)

ABSTRACT

The experimental modelling of a gas-liquid-liquid downward flow in a vertical pipe was performed to characterize the transportation of CO2 for further industrial application of the flow process. The study involved a multiphase downward flow pipe model integrated with a high-speed video camera to observe the flow patterns developed from the experimental proceedings of the flow process. This was achieved by varying the input flow rates of the CO2 gas phase at high, medium and low set water-cuts values of the liquid phases. These flow patterns were observed for 0.452 to 32.868m/s range of the calculated superficial velocities of the gas phase. The homogenous water and kerosene liquid phase was found between 0.452 to 32.868m/s 0.008 to 13.0734m/s at 20, 50, 70 and 90% water-cuts. Subsequently, the relationship between the area fraction occupied by the gas phase, the calculated superficial velocities of the gas and the homogenous liquid phases were utilised to empirically predict the transition criteria of one flow pattern to another for the developed flow pattern map of the studied flow system. These findings provide an adequate understanding of the industrial transportation, carbon capture and underground sequestration of CO2 gas through a three-phase downward flow in the pipe; to meet the demands of emerging technologies..

Keywords: *Three-phase, Flow Patterns, Water-cuts, Gas radius, and Superficial velocity*

1.0 INTRODUCTION

The idea of multiphase flow in pipes is to accurately predict the flow behaviour of complex flow systems for economical and safe transportation of fluids. A three-phase flow structure is more complicated than a two-phase flow structure (Farman and Yeung, 2005). The research by Bannwart et., al. (2009) showed that the development of specific flow patterns indicates how the phase distributions affect the physical nature of the flow system. This classification depends on variables of the operating condition, such as the fluid properties, flow parameters and the pipe orientation and geometry. These patterns are represented in a map to characterise the flow process of a system.

According to Alipchenkov *et.,al.* (2004), a flow pattern map is a means to technically analyse the flow characteristics of a multiphase flow system and establish the boundary conditions of the developed flow patterns. It defines the flow parameters responsible for forming the observed flow patterns and develops guiding principles for a flow system. Huang *et., al.* (2013) study on the flow pattern map for air-water-heavy oil three-phase upward flow in a vertical pipe considered the various flow patterns formed at very low phase velocity of the multiphase fluids in the vertical pipe. The experimental observations further established eleven typical flow patterns: mist, bubble, slug, churn, annular, and wavy or disperse. However, the usual way of developing a flow pattern map is to identify the certain flow conditions of a flow system and then predict the transition criterion of one flow pattern to another through a boundary line (Taitel & Dukler 1990). Thus, the flow pattern maps of Zangana (2011) described the usual way of developing a flow pattern map, identifying certain flow conditions of a flow system, and predicting the transition criterion from one flow pattern to another. Furthermore, Almabrok *et., al.*(2015) work revealed that the flow pattern map and its predicted transition criterion vary over the different multiphase flow systems, such as the fluid materials and the pipe characteristics.

Conversely, the flow pattern transition criteria are the conditions that must be attained for a possible transition from one multiphase flow pattern to another (Benjamin *et., al.* 2017). They are attributed to the changes in the physical characteristics of the multiphase flow process. A typical example was observed by Rau *et., al.*(2016), when turbulence forces shattered the big gas bubbles and coalesced into slugs to transition from Bubble to Slug flow pattern. The Bubble to Slug transition was mainly observed in their study at low liquid velocities. However, as the flow turbulence increased due to the higher liquid velocity in the system, smaller equilibrium bubbles were developed for the Slug to Churn flow pattern transition process (Kong *et., al.* 2018). According to Piela *et., al.* (2019), this flow process was best described as the upper limit of the slug region due to the flooding of the gas bubble and that of the liquid film separating the bubble from the pipe wall. This flooding

Copyright© College of Engineering and Engineering Technology

phenomenon causes the breakup of the long vapour bubbles that produce a Churn flow pattern. The study of Kong *et., al*. (2018) further revealed that the Churn to Annular flow pattern will take place in a flow system if the gas velocity is just enough to suspend droplets on the pipe surface; where the Disperse flow pattern occurs when the turbulence of the continuous gas phase is "sufficiently intense" to break the liquid phase into droplets smaller than the critical size. These observations made over years of study of multiphase flow in pipes have proved the experimental modelling technique to be an accurate means of analysing the flow characteristics of the flow process. The experimental modelling techniques, often employed by researchers, utilised the measured flow parameters to describe the observed flow patterns of the multiphase flow process. These flow parameters were further used to predict the transition criterion of the flow pattern map for a multiphase flow in pipes (Taitel and Dukler1990). For example, in the experimental study of three-phase bubble flow in vertical pipes by Piela *et., al*.(2009), the average volumetric concentration of the gas phase was predicted as a function of the distribution parameter and the average drift velocity of the multiphase flow. Depending on its application, recent studies have employed different analytical approaches of experimental models to predict the transition mechanism of one flow pattern to another and general characterisation of the flow phenomenon. They include the homogenous, separate or drift-flux flow system.

The homogeneous flow approach assumes the multi-phases are well mixed and travelling with the same velocities; hence, they are treated as a single fluid (Oddie *et., al.* 2003). However, study by Shi *et., al.*(2015) considered their flow process to be separated with the restriction on equal phase velocities is relaxed, and each phase is assumed to be flowing in its pipe. The drift-flux model analyses a flow system with different superficial velocities flowing in a pipe, with an additional constitutive equation for the closure relationship interfacial force (Omebere-iyari 2019). This force accounted for the shear stress and the slip velocity between the phases to improve accuracy and applicability. However, the volume of fluid (VOF) analytical approach applied in the flow model of (Zangana 2011) defined the fraction occupied by the volume of each phase in the pipe by solving a single set of momentum equations of the flow process.However, despite the versatility of these modelling techniques, multiphase flow in pipes is limited to liquid-liquid or gas-liquid upward flow to meet industrial demands. Therefore, it is necessary to investigate the introduction of new fluid in a multiphase process to achieve more than one objective rather than modifying existing ones. Hence, in an oil and gas reservoir, the need to sequestrate greenhouse emitted gas in a three-phase flow system will simultaneously enhance the recovery of oil and lighter natural gas production processes, while harmful heavier gas, such as CO_2, is captured underground. This paper presents the flow pattern map developed by introducing CO_2 gas in a gas-liquid-liquid flow in the pipe. The experimental model was designed to perform the simultaneous downward flow of the three phases in a vertical pipe with the objective: to utilise the calculated superficial velocities of the phases to characterise the developed flow patterns of the flow process. The findings will provide improved cost-effective, environmentally-friendly oil and gas production flow systems to meet future industrial demands of emerging technologies.

2.0 MATERIALS AND METHODS

The experimental model was designed for a three-phase downward flow of fluids in a vertical transparent pipe to obtain the measured flow parameters of the developed flow patterns that will characterise the flow process of the system.

2.1 Materials

The basic materials used were steel metal, polyvinyl chloride (PVC) pipe, gas and liquid storage chambers, yellow ink, pressure gauges, flow meters, flow valves, and a high speed (HP CW450t) digital camera with a shutter speed of 1/250. The fluid properties of CO_2 gas, kerosene and water; and the instruments' characteristics are presented in Tables 1 and 2.

Table 1: Fluid properties at 25°C

Fluid/Phase property	Water (w)	Kerosene (o)	CO_2 Gas (g)
Density, ρ (kg/m^3)	997.80	810.12	1.98
Viscosity, μ $(N.s\ m^{-2})$	0.000891	0.00216	0.0000625

Table 2: Characteristics of the experimental instruments

S/N	Measured data	Manufacturers specification	Range	Uncertainty (U_{ai})

1	Liquid flow rate (m^3/sec)	Digital flow meter	0 to 35	± 0.002
2	Gas flow rate (m^3/sec)	Digital flow meters	0 to 35	$\pm$ 0.001
3	Pressure (Bar)	Digital pressure gauge	0-10	± 10

2.2 Methods

The experimental design consists of a frame of 3.61m length, 0.9m wide, and 0.9m breath of steel material coated with white paint to enhance the visibility of the experimental observations. As shown in Fig. 1, the oil and the yellow inked water liquid phases were stored in two tanks of 0.2 m^3 capacity, respectively. In contrast, the CO_2 gas phase was stored in a 2.5m^3 gas cylinder at 101.3KPa pressure. Subsequently, 0.0315m and 0.0127m inner diameter transparent PVC pipes attached with flow meters were fixed at the outlet for the storage compartments of the liquids and the gas phases respectively. These pipes, as shown in Fig. 2(a) and (b), were connected from the top of a 2.201m length L and 0.0508m internal diameter d_m transparent PVC test-section pipe, through the regulated valves, at 0.2 m, 0.3 m and 0.4 m for the oil, water and CO_2 phases. Further, the top of the test-section pipe of the experimental set-up, as captured in Plate 1 was sealed at the top, and the outlet below was connected to a recovery tank.

2.2.1 Experimental Procedures

The experimental modelling technique applied to characterise the flow parameters of the flow system was based on the governing laws of continuum mechanics and dynamics for the conditions that the studied flow process was incompressible, steady and in a one dimension-constant energy state. The experimental procedure was to simultaneously open the valves for the oil and yellow-inked water input pipes to allow the homogenous flow of a set water-cut value of the liquid phase, while the CO2 gas-phase input pipe valve was varied to achieve a full and stabilized flow of the three phases down the test-section pipe. Consequently, the observed yellow inked flow pattern of the flow process developed in the test section pipe was captured by a high speed (HP CW450t) digital camera with a shutter speed of 1/250, while the measured input flow rate readings of the three phases were subsequently recorded. These experimental procedures were repeated accordingly, where the gas input flow rate was varied for the different set WCs values of the liquid phase. The hydrodynamic water-cut (WC) characterisation of a liquid is defined as the volume percentage of water in a multiphase flow system. The volume of fluid (VOF) analytical approach of the experimental model was to replicate the liquid-liquid WCs flow processes obtained in existing multiphase petroleum recovery pipe systems; hence, this experimental study was performed for a low, medium and high WCs set values at 20, 50, 70 and 90%.

2.2.2 Calculation of the three-phase flow parameters

The uncertainty analysis for a measured flow rate of fluid in pipes [7] was adopted and applied for this study. The absolute measured flow parameter q_a for each phase was determined using equation (1).

$$q_a = \sum U_a + q_{ai}; \quad (1)$$

The values of U_a was determined using equation (2)where U_a, U_{ai}, $q_{ai}$and n are the total uncertainty, the uncertainty variable, the measured input flow rate, and the number of total uncertainty variables. The subscript a was used for each considered phase.

$$U_a = \left[\sum_{i=1}^{n} \left(\frac{\partial q_{ai} + U_{a_i}}{2}\right)^2\right]^{\frac{1}{2}} \quad (2)$$

Hence, for the study of the three-phase downward flow in a vertical pipe system, the expression for the total volumetric flow rate (q_m) of the flow process was evaluated using equation (3); where subscripts $o, w \; and \; g$ represents the oil, water and gas phases.

$$q_m = q_o \sin\emptyset + q_w \sin\emptyset + q_g \sin\emptyset; \quad (3)$$

The values of the set hydrodynamic WC of the liquid phase were determined using equation (4)

$$\text{Water-cut, WC} = \frac{q_w \sin\emptyset}{q_o \sin\emptyset + q_w \sin\emptyset} \times 100\% \quad (4)$$

Subsequently, the calculated input phase and the superficial velocities of the oil, water and gas phases were evaluated using equations (5) and (6), respectively; while the superficial velocity of the homogenous liquid phase v_l was further calculated in equation (7); where A_{io}, A_{iw}, A_{ig} and $A_m$were the respective cross-sectional areas of the input pipes for the phases, and A_m was the cross-sectional area of the test section pipe.

$$V_o = \frac{q_o \sin\emptyset}{A_{io}}; \quad V_w = \frac{q_w \sin\emptyset}{A_{iw}}; \quad V_g = \frac{q_g \sin\emptyset}{A_{ig}} \quad (5)$$

$$v_o = \frac{V_o \ A_{io}}{A_m}; v_w = \frac{V_w \ A_{iw}}{A_m}; v_g = \frac{V_g \ A_{ig}}{A_m} \quad (6)$$

$$v_l = v_o + v_w \quad (7)$$

Generally, the studied three-phase downward flow process was considered as a homogenous liquid (combined water and oil phases), and a separate gas phase in the test-section pipe. Hence, the calculated superficial gas and the homogenous liquid velocities were utilised to characterise the observed flow patterns captured at 20, 50, 70 and 90% water-cut values.

2.2.3 Procedure for the development of the flow pattern map

The volume of fraction drift-flux analytical method was applied to determine the volume fractions (VOF) $\alpha_l \ and \ \alpha_g$ for the liquid and the gas phases as:

$$\alpha_l = \frac{v_l}{v_m}; \quad \alpha_g = \frac{v_g}{v_m} \quad (8)$$

However, as there was no mass exchange or chemical reaction among the phases, the continuity mass balance equation in terms of the volume fractions for the three-phase flow process must meet the expression of equation (9)

$$\alpha_l + \alpha_g = 1 \quad (9)$$

Hence, the calculated value for the area of flow $A_g$and the radius fraction R_g of the gas phase in the test section pipe was derived in equation (10); while the area fraction *h* occupied by the gas phase in the test-section pipe was calculated using equations (11).

$$A_g = \alpha_g A_m; \text{and} R_g = \sqrt{\frac{A_g}{\pi}} \quad (10)$$

$$h = \frac{R_g}{R_m} \quad (11)$$

Further, an empirical analysis that utilised the area fraction occupied by the gas phase and the calculated flow parameters of the flow process was performed to determine the transition criteria of the developed flow patterns for the studied WCs. The following cases of the area fraction were applied for the calculated superficial velocity of the flow process as follows:

Case:

i. When $h \ll 1$: the liquid phase occupied the pipe as the continuous phase, while the large gas bubbles collide to form slugs in the pipe at $v_l \geq v_g$.
ii. When $h \leq 1$: the gas velocity was increased, thereby resulting in the value of the ratio of gas radius to the radius of the test section rising towards 1; where the Churn flow patterns were observed at $v_g > v_l$.
iii. When $h = 1$: the flow became Annular with a gas phase flowing at the core of the pipe diameter at $v_g \gg v_l$.
iv. When $h \geq 1$: the gas occupied in the pipe becomes Disperse droplets in the liquid phase at $v_g > 2v_l$.

3.0 RESULTS AND DISCUSSION

3.1 Results of the observed flow patterns and the calculated flow parameters

The experimental proceduresperformed for the calculated superficial flow velocities rangefor the multiphase flow processwere found to range from 0.452 to 36.671m/s and 0.008 to 4.952m/s for the CO_2 gas and the homogenous liquid phases, respectively. The captured developedBubble, Slug, Churn, Annular and Disperse flow patternsfor the studied flow process at the set water-cuts WCs were presented in Fig. 3

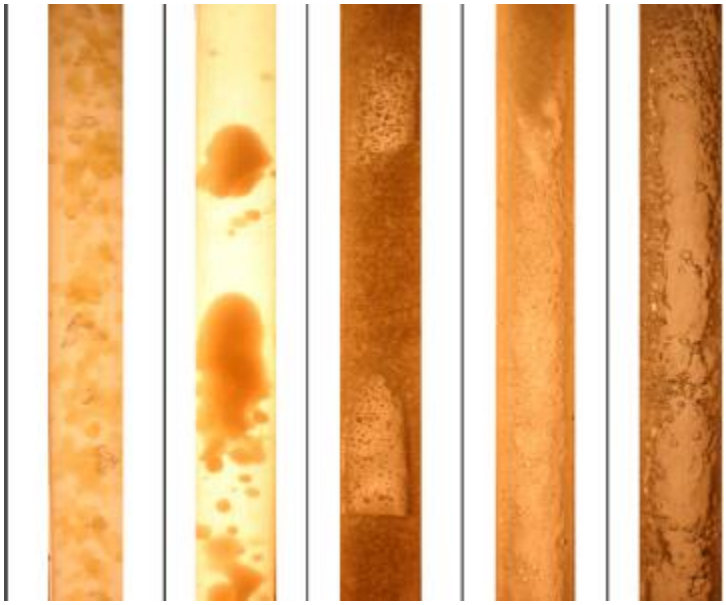

Fig. 3: Captured flow patterns of studied three-phase downward flow in a pipe.

3.2 Representation of the flow patterns

At 20% WC, the Bubble flow pattern was observed at low superficial liquid and gas velocities calculated at 0.201 ≤ v_l ≤ 2.723 and 0.152≤ v_g ≤ 1.674m/s. The captured flow pattern was similar to the large shaped bubbles formed close to the sphere of the pipe observed by (Oddie *et., al* 2003). Also, Rau *et., al*. (2016) explained that the spatial cross-sectional distribution of the gas phase void fraction caused the Bubble flow pattern. However, this study showed that this flow pattern was developed when the liquid cross-sectional average velocity was higher than gas. Subsequently, as the superficial gas velocity was increased, the clusters of the gas bubbles collided together to form larger patches of bubbles randomly distributed in the continuous liquid phase dominated multiphase flow for a Bubble/Slug (BS) flow pattern at 1.5 ≤ v_g≥ 1.5m/s. Subsequently, the Slug flow pattern was fully observed at 2.471 ≤ v_g≤ 6.755m/s when the liquid phase velocity was maintained at 0.245 ≥ v_l ≤ 2.624m/s. This was in line with Kong *et., al.*(2018) results that described Taylor's bubbles to form a dense foam region as they flow downwards in the pipe. As shown in Fig. 4, the Slug/Churn (SC) flow pattern was observed at v_g≥ 7.1m/s; and then to a full Churn flow pattern that covers the largest portion of the flow process at 8.701≤ $v_g \geq 18.317$m/s. The flow process was similar to the results captured by Oddie *et.,al.* (2003), which described the faster influx of gas in the fluid mixture as a spherical patch of the multiphase flow process. Further increase in the gas velocity to $v_g \geq 20.876$m/s resulted in the Annular flow pattern; while the Disperse flow pattern was observed for all values of regulated superficial gas velocity at $v_l \geq$ 3.6m/s.

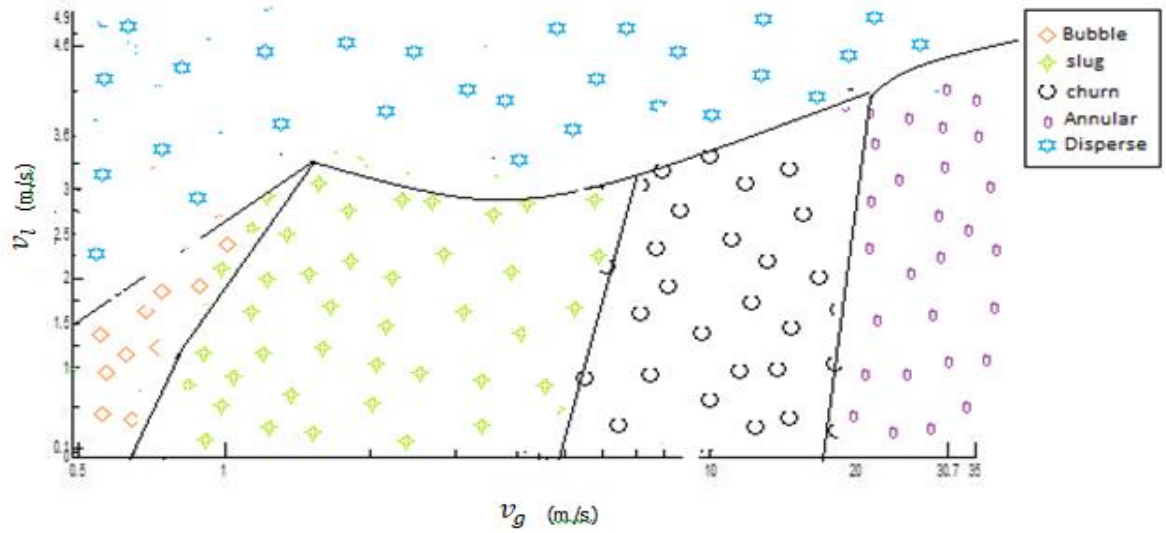

Fig. 4: Representation of the flow patterns at 20% WC

The representation of the Bubble flow pattern in Fig, 5 showed that it was developed for the range of the gas velocity of 0.152≥ v_g ≤ 0.564m/s for the 50% WC of the studied flow process. This observation was made when the ease of bubble formation fusion was attributed to the less viscous nature of the homogenous fluid mixture. According to Hanafizadel *et.,al.* (2017) the coalescence of the bubbles can happen more readily because of the lack of relative motion between the gas and the liquid phases. However, unlike the 20% WC, the Slug and the Churn flow patterns were observed at 0.152 ≥ v_g≤ 6.86m/s and 7.991≥ v_g≤ 19.98m/s for the liquid phase velocity at 0.118 ≤ v_l ≤ 3.530m/s. Omebere-Iyari and Azzopardi (2019) justified that the reason for this rapid change was due to the less viscous nature of the fluid mixture, thereby causing early turbulence of the multiphase flow in the pipe. Further increase of the superficial gas velocity to v_g≥ 20.510m/s resulted in the Annular pattern; while the Disperse flow pattern was observed at v_l≥ 3.510m/s:The representation of the studied flow process in Fig. 5 for the 50% WC revealed that the superficial gas velocity was far greater than the liquid phase (v_g ›› v_l).

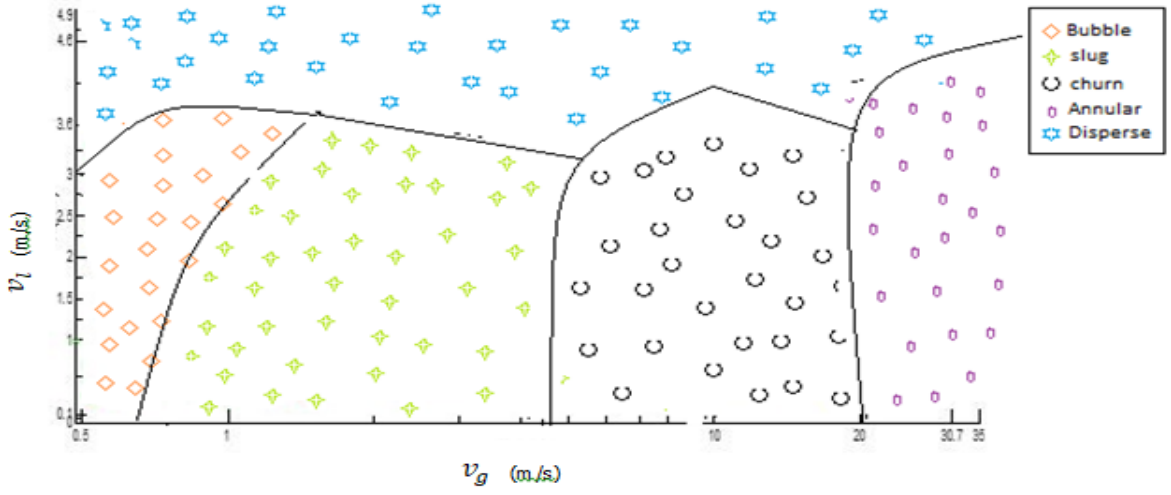

Fig. 5: Representation of the flow patterns at 50% WC

However, the 70% WC flow process shown in Fig. 6 indicated a change in the superficial velocity profile for the developed flow patterns due to the higher water phase volume in the multiphase flow. The largest range of the Bubble flow pattern when compared to other WC values was observed at 0.152 ≤ v_g≤ 1.712m/s, and 0.108 ≥v_l≤ 3.891m/s. The Slug flow pattern was observed at 1.812 ≤ v_g≤ 9.920m/s; while a high velocity of the gas phase was measured for the Churn at 8.178 ≤ v_g≤ 24.320m/s. These observations were similar to Zhao *et., al.* (2016) results that described the churn formation as a continuous layer of water in the flowing oil mixture, with droplets of gas entrained due to the high volume fraction of the water phase occupied in the multiphase flow process. The Annular flow pattern was observed atv_g ≥ 26.12m/s for 0.138 ≤ v_l≤ 3.720m/s. This flow pattern resulted fromthe higher gas phase velocity as the gas occupied the core of the test tube with the oil film wetting the pipe wall (Puela *et., al.* 2009). Further increase of the superficial gas velocity to v_l ≥ 4.02m/s resulted to the formation of the Disperse flow pattern. At 70% WC, the description of this flow pattern was observed to flow as a rippling wave with tiny gas bubbles entrained in the liquid phase. This observation as explained by Zangana (2011) was due to the effect of the gravitational force on this flow process. The result of the 70% WC of the studied flow process was characterised as a water-based film containing small oil and gas droplets continuously wet the pipe perimeter.

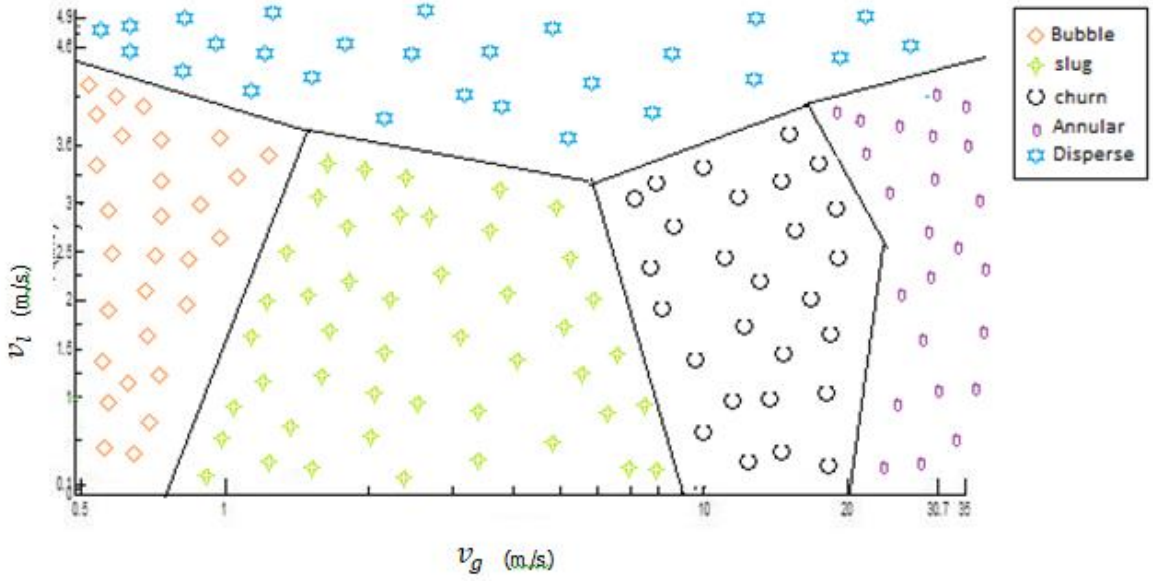

Fig. 6: Representation of the flow patterns at 70% WC

Further, the 90% WC of the studied flow process had a unique flow process where the Bubble flow pattern was observed at 0.109 ≤ v_g≤ 1.296m/s and 1.545 ≤ v_l ≤ 4.923m/s as the gas volume fraction was reduced to 0.2. Consequently, due to a very high volume fraction of water in the liquid phase, the Slug flow pattern shown in Fig. 7 was observed at 0.455 ≤ v_g ≤ 4.591m/s; and the Churn flow pattern at the range of 5.272 ≤ v_g ≤ 20.711m/s; as the superficial homogenous liquid velocity remain constant. Also, similar to Kong *et., al.* (2018), these flow patterns develop faster in a less viscous liquid phase when waves fluctuate at the liquid/gas interface with small liquid drops entrained in the pipe. The Annular flow pattern was evident when all the phases flow separately; as the gas phase occupies the pipe core at v_g ≥ 21.925m/s with the oil droplets on the wall of test-section pipe an increase to v_l ≥ 4.553m/s However, further increase of the liquid homogenous velocity to v_l ≥ 4.953m/s resulted to the Disperse flow pattern; where tiny bubbles of the liquid phase dominate the studied flow process. According to Rochaa *et., al.* (2017), the characteristics of these flow processes at 90% WC can be explained as the separation of the water and the oil phases due to the pressure gradient of the effects of the gravitational and shear forces at a high water velocity.

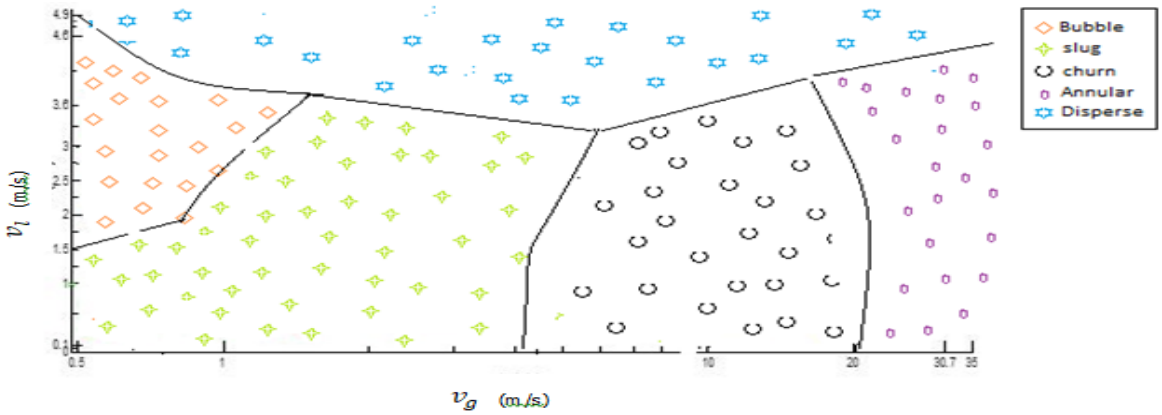

Fig. 7: Representation of the flow patterns at 90% WC

3.3 Development of the Flow Pattern Map

The volume of fluid (VOF) drift-flux analytical approach was applied to achieve low, medium and high set hydrodynamic water-cut (WC) values of 20, 50, 70 and 90% of the liquid phase flow. This established the calculated volume fraction of the homogenous liquid and the gas phases for the set WCs of the studied flow process.

Table 1. The results of the calculated values for the area fraction occupied by the gas phase; and the superficial velocities of the homogenous liquid and gas phases

	20% WC			50% WC			70% WC			90% WC		
v_g (m/s)	v_l (m/s)	*h*	Flow Pattern	v_l (m/s)	*h*	Flow Pattern	v_l (m/s)	*h*	Flow Pattern	v_l (m/s)	*h*	Flow Pattern
0.452	0.0401	0.4330	B	0.1059	0.5535	B	1.1668	0.4594	B	1.3211	0.4594	B
1.615	0.1826	0.7086	S	0.3237	0.7883	S	1.7594	0.6992	BS	2.4130	0.6992	BS
5.348	0.2455	0.9055	S	0.4821	0.9141	SC	2.0200	0.8716	S	3.1191	0.8716	S
7.513	0.3317	0.9055	SC	0.6474	0.9188	SC	3.3782	0.9035	SC	4.2821	0.9035	SC
12.51	0.4976	0.9448	C	0.8748	0.9417	C	4.0696	0.9385	C	4.5487	0.9385	C
15.82	0.6393	0.9448	AC	1.3137	0.9687	C	4.8576	0.9503	C	4.8989	0.9503	C
20.34	0.9438	1.0001	A	3.6869	0.9790	CD	4.5257	0.9748	CD	4.3071	0.9748	CA
24.87	1.2366	1.0001	A	2.4918	0.9993	A	5.9434	0.9998	A	9.6588	0.9999	A
29.56	4.6812	1.0118	AD	4.2646	1.0087	A	4.9984	1.0027	AD	13.1042	1.0027	AD
32.67	4.8157	1.0196	D	4.6059	1.0196	AD	7.5521	1.0035	D	14.4195	1.0035	D

Copyright© College of Engineering and Engineering Technology

The empirical analysis result utilised the relationship between the calculated area fraction occupied by the gas phase; and the superficial velocities of the homogenous liquid and gas phases for the studied WCs shown in Table 1 to correlatethe flow patterns transition criteria of the three-phase flow process.

(i) Bubble-Slug Transition Criterion (B-S): The results revealed that the transition from Bubble to Slug flow occurred at$h$ = 0.717for the range of the homogenous liquid mixture velocity of 4.545 ≤ v_g ≤ 16.921m/s. These were observed at v_g ≤ 1.0921m/s for 20 and 50% WCs and at v_g≥ 1.956m/s for the higher WCs, where v_l≤ 3.456m/s to satisfy the criterion for Case 1. The result is in line with the study by Benjamin *et., al*. (2017), which reported the transitions between the bubble and slug flow were observed when the large bubble clusters of the flow process coalesced into slugs; usually when the inlet velocities of the liquid were far greater than the velocity of the gas phase. Also, Mishima and Hibiki (2016) revealed that the Bubble to Slug transition criterion usually develops at a low gas velocity compared to other flow patterns. Hence, the calculated flow velocities analysed to satisfy the case of $v_l \gg v_g$at $h \ll 1$.

(ii) Slug-Churn Transition Criterion (S-C): The superficial gas velocity for the transition from Slug to Churn flow patterns was within 4.545 ≤ v_g ≤ 6.921m/s for all WCs. However, the maximum superficial velocities of the homogenous liquid phases were found at v_l ≤ 4.25, satisfying Case 2, where $v_g \geq v_l$at $h \leq 1$. This was also supported in Mishima and Hibiki. (2016), the study revealed that distinguished the Slug from the Churn flow pattern as to when the gas phases become the driving momentum of the multiphase flow process. In the studied flow process, the transition occurred like a complicated wave structure appearing in the pipe

*(iii) Churn-Annular transition Criterion (C-A):*The Churn-Annular transition was established for all WCs to meet the CASE 3 of h = *1* at $v_g \gg v_l$ where the multiphase flow process was observed to be less viscous due to the high velocity of the gas phase. The process took place within the range of the gas and homogenous liquid velocities at $7.754m/s \geq v_g \leq 21.32m/s$and $3.03m/s \geq v_l \leq 3.72m/s$. Accordingly, Raul *et., al.*(2016) reported that a Churn/Annular flow pattern with a distinct tail was observed in the pipe of a less viscous multiphase flow process; thus, revealing that the gas phase velocity was responsible for the multiphase flow pattern transition process.

(iv) Annual-Disperse Transition Criterion (A-D): The Disperse flow occurred where one phase of the multiphase flow process was fully or partially dispersed Loverick and Angeli (2004). Subsequently, Schmidt et., al. (2008) described the transition when the effects of turbulence overcome the surface tension distribution among the phases in a multiphase flow process. Hence, this transition occurred for the studied multiphase flow process at $v_l \geq$ 2.821m/s; where CASE 4 of $h > 1$ at $v_g > 2v_l$ was achieved for all WCs. The studied multiphase flow process was observed to become fully dispersed, with the tiny gas droplets occupying over 80% of the pipe volume at a very gas phase velocity. These observations were supported by the study of Descamps *et., al.* (2016)that revealed the dispersed flow pattern to develop at a higher gas velocity than the liquid phase.

The correlated empirical developed results of the flow patterns transition criteria at the studied WCs were applied to develop the flow pattern map of the system. The flow pattern map of the studied flow process presented in Fig. 8 revealed that the Bubble flow pattern was observed for the gas velocity from 0.152 to 2.521m/s for the range of the liquid velocity from 0.281 to 3.321m/s. The Slug and the Churn flow patterns were developed at 3.152 ≤ v_g ≤ 7.671m/s and 2.521 ≤ v_g ≤ 21.192m/s; for 0.281 ≤ v_l ≤ 4.798m/s. The core gas-phase annular flow pattern was fully formed for the gas and liquid velocities from 22.682 to 41.347m/s and 0.281 to 5.121m/s. Further increase of the homogenous liquid superficial velocity from 2.846 to 5.216m/s resulted in the Disperse flow pattern formation. Hence, the flow pattern map for applying CO_2 gas in a three-phase downward flow in the pipe was developed for the operating flow parameters of 0.152 ≤ v_g ≤ 40.671m/s and 0.281 ≤ v_l≤ 5.216m/s for the gas and the homogenous liquid superficial velocities. However, it is important to note that every multiphase flow process has a unique flow pattern map, whether it is empirically correlated or numerically developed (Benjamin *et., at.* 2017). Their variance depends on the physical properties of the applied fluid materials, the pipe dimensions, and the considered flow parameters and conditions of a given system; where it serves as a guide to technically analyse the flow characteristics for a peculiar multiphase flow system. Hence, the flow pattern map for the application of CO_2 in a three-phase downward flow in a pipe presented in Fig. 8 was developed as a guide to analyze the relationship between the calculated superficial velocities and the calculated area fraction of the phases of the studied flow process from the correlated flow patterns transition criteria at 20, 50, 70 WCs.

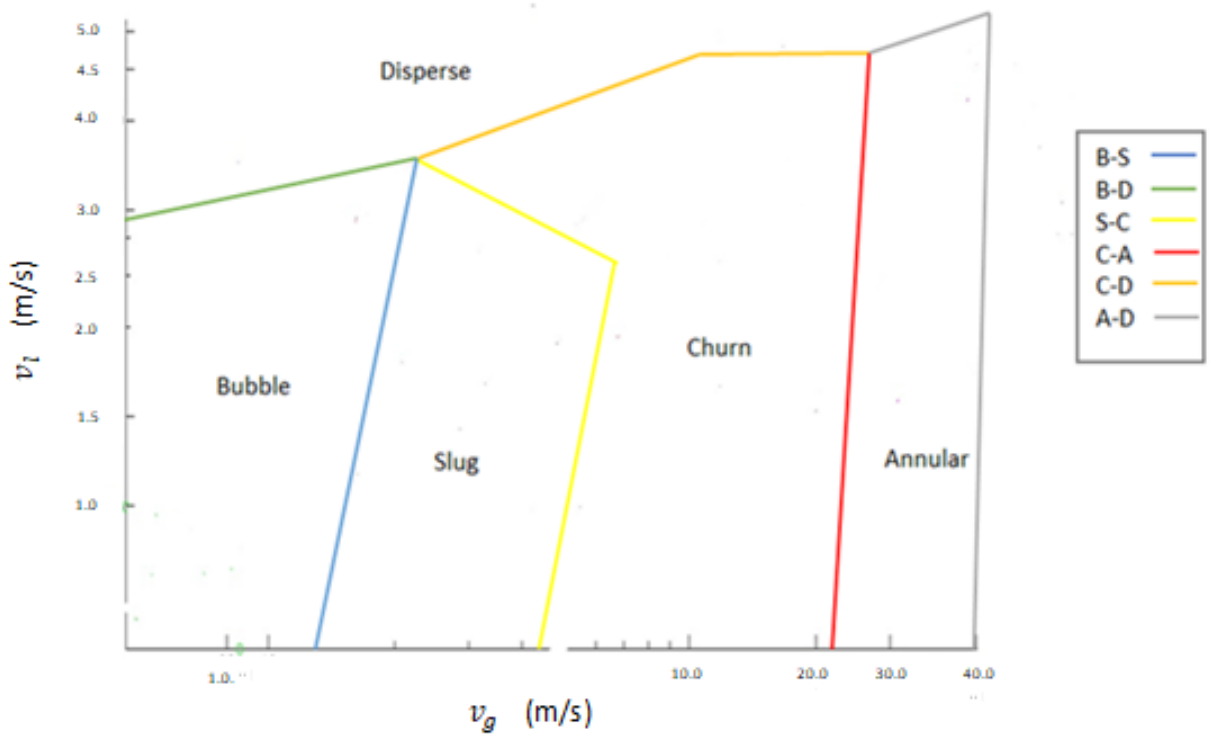

Fig. 8: Flow pattern map of the studied flow pattern model

4.0 CONCLUSION

The experimental study results for applying of CO_2 in a gas-liquid-liquid multiphase downward flow in a vertical pipe revealed the development of the Bubble, Slug, Churn, Annular, and Disperse captured flow patterns. These developed flow patterns were observed at the set 20, 50, 70, and 90% WCs of the flow process for the range of homogenous liquid and the superficial gas velocities from 0.281 to 5.216m/s and 0.152 to 40.671m/s. Subsequently, a relationship between the superficial velocities of the phases and the area fraction occupied by the gas phase *h* was established to empirically predict the flow patterns transition criteria of the flow process. The correlated transition criteria results for set WCs were revealed for Bubble to Slug (B-S) at $h \ll 1$ for $v_l \gg v_g$; Slug to Churn (S-C) at $h \leq 1$ for $v_g \geq v_l$; Churn to Annular (C-A) at $h = 1$ for $v_g \gg v_l$ and Annular to Disperse (A-D) at $h > 1$for $v_g > 2v_l$. Theseresults were utilized to develop the flow pattern map for operating flow velocities of the studied flow system. Hence, the flow pattern map development was established as an operating working guide that characterized the application of CO2 gas in a three-phase downward flow in a pipe to meet emerging technologies.

References

Farman Ali, H. Yeung, (2005) Experimental Study of Two-Phase Air-Water Flow in Large Diameter Vertical Pipes, Chemical Engineering Communications 202: pp. 823-842

Bannwart, A.C., Rodriguez, O.M.H., Trevisan, F.E., Vieira, F.F., De Carvalho, C.H.M., (2009). Experimental investigation on liquid-liquid-gas flow: Flow patterns and pressure- gradient. Journal of Petroleum Science and Engineering, 65(1): pp. 1–13

Alipchenkov, V.M., Nigmatulin, R.I., Soloviev, S.L., Stonik, O.G., Zaichik, L.I., Zeigarnik,. (2004). A three-fluid model of two-phase dispersed annular flow, International Journal of Heat and Mass Transfer 47: pp. 5323-5338

Huang, S. (2013). “Study on flow pattern maps in air–water–oil three-phase flows”. Experimental Thermal and Fluid Science, 67: pp. 158-171

Taitel, D. Barnea, Dukler A.E, (1990). “Experimental Model and prediction of the flow pattern transitions for

steady upward gas-liquid flow in vertical tubes". *AIChE J*. 26:pp 345–354.

Zangana, M. H. S, (2011). Film behaviour of vertical gas-liquid flow in a large diameter pipe.*PhD thesis, The University of Nottingham.*pp. 76.

Almabrok A. Almabrok , Aliyu M. Aliyu , Liyun Lao , Hoi Yeung (2015), "Gas/liquid flow behaviour in a downward section of large diameter vertical serpentine pipes, *International Journal of Multiphase Flow12: 87 – 98.*

Benjamin Wu, MahshidFirouzi, Travis Mitchell, (2017). "A critical review of flow maps for multiphase flows in vertical pipes". *Chemical Engineering Journal,* 326, pp. 350–377

Rau, A., Kong, R., Kim, S., Bajorek, S., Tien, K., Hoxie, C. (2016). "Image analysis for bubbles developed in a horizontal multiphase flow". *Proceedings of 2016 ANS Winter Meeting, November Las Vegas, NV USA*: pp. 1512–1513.

Kong, R., Rau, A., Kim, S., Bajorek, S., Tien, K., Hoxie, C., (2018)."Experimental study of horizontal air-water slug-to-churn transition flow in different pipe sizes". *Int. J. Heat Mass Transfer123:*pp.1005–1020.

Piela, K., Delfos, R., Ooms, G., Westerweel, J., Oliemans, R.V.A. (2009). "Annular and Dispersed oil– water–gas flow through a horizontal pipe". *AIChE J. 55:* pp *1090–1102.*

Oddie, G., Shi, H., Durlofsky, L.J., Aziz, K., Pfeffer, B., Holmes, J.A., (2003). "Experimental study of homogenous two and three-phase flows in large diameter inclined pipes". *International Journal of Multiphase Flow, 29(4):* pp. 527-558

Hanafizadeh P., A. Shahani, A. Ghanavati, Akhavan-Behabadi M.A. (2017) "Experimental Investigation of Air-Water-Oil Three-Phase vertical Flow Patterns in vertical and Inclined Pipes. *Experimental Thermal and Fluid Science 10*: pp. 1016

Shi, H., Holmes, J., Durlofsky, L.,Aziz, K., Diaz, L., Alkaya B., Oddie, G., (2015). "Drift-Flux Modeling of Two Phase Flow in Wellbores".*SPE Journal 10:* pp. 24-33.

Omebere-Iyari N.K., Azzopardi B.J., (2019). "A drift-flux Study of the Developed Flow Patterns for Gas/oil/Liquid Flow in Small Diameter Tubes", *Chemical Engineering Research and Design* 85:pp. 180- 192.

Zhao, J.F. Xie, J.C Hu, H, Ivanov, I, and A.Y. Belyaev. (2010). "Experimental studies on two-phase liquid-liquid flow patterns". *International journal of multiphase flow, 27(11):* pp. 1931–1944.

RochaaD.M , Carlos H. M. de Carvalhob , Estevamc V., Oscar M. H. Rodriguezd (2017). "Effects of water and gas injection on the volumetric fraction and the pressure gradient in upward-vertical three-phase pipe flow". *Journal of Petroleum Science and Engineering, 157:* pp. 519–529

Mishima, K., Hibiki, T., (2010)."Some characteristics of air–water and low viscous flow in small diameter vertical tubes".*Int. J. Multiphase Flow 22:* pp. 703–712.

Lovick, J., Angeli, P., (2004). "Experimental studies of the disperse continuous flow pattern in air-oil-water flows". *Int. J. Multiph. Flow 30,* pp. 139–157.

Schmidt, J.; Giesbrecht, H.; van der Geld, C.W.M. (2008)."Analysis of the Phase and velocity distributions in vertically upward two-phase flow map".*Int. Journal on Multiphase. Flow vol. 34:* pp. 363–374.

Descamps, M.N., Oliemans, R.V.A., Ooms, G., Mudde, R.F., (2010). "Air–water flow in a vertical pipe: experimental study of air bubbles in the vicinity of the wall". *Exp. Fluids* 45: pp. 357–370.